

The nonlinear dispersion relation of geodesic acoustic modes

R. Hager, K. Hallatschek

Max-Planck-Institut für Plasmaphysik, Garching b. München, Germany

Introduction. The turbulence determines the distribution of geodesic acoustic mode (GAM) activity in real and in Fourier space by modifying the radial propagation velocity and setting the radial scale of the turbulent excitation of GAMs. Therefore, the interaction between turbulence and GAMs is crucial for the understanding of the experimentally observed frequencies, e.g. the frequency plateaus observed in ASDEX Upgrade (AUG) [1]. It may also play a role in the explanation of the pulsating GAM activity found recently during the I-phase in AUG [2] or the periodic turbulence suppression in NSTX [3]. Furthermore, fast GAM propagation – representing a special form of damping – would have to be taken into account when considering the excitation of GAMs by external coils.

Nonlinear GAM dispersion. Figure 1 shows the result of a nonlocal two-fluid ITG turbulence computation (non-adiabatic electrons) with circular flux-surfaces obtained using NLET [4] with $\lambda \approx 200$, $\eta_i \equiv L_n/L_{T_i} = 2.4$, $\eta_e \equiv L_n/L_{T_e} = 0$, $\varepsilon_n \equiv 2L_n/R = 0.05$, $\alpha_d = 0.5$, $\varepsilon_v = 0$, and $\gamma_p = 0$ (definitions in [4]). The radial variation of the GAM frequency caused by non-locality is obvious in the corresponding $\mathbf{E} \times \mathbf{B}$ -flow profile [Fig. 1 a)]. Its temporal Fourier transform [Fig. 1 b)] reveals that GAMs with frequency $\omega_{GAM,0}(r_0)$ (indicated by the dashed line) radiate significantly outwards to $r > r_0$ but disappear for $r < r_0$. The application of a narrow band pass filter [Fig. 1 c)] shows that the flow profile consists of *global* GAM eigenmodes. Such an eigenmode can be regarded as a WKB wave packet with a local wave number k_r obeying $\omega_{GAM}(r, k_r) = \text{const.}$ To relate the observed deviations from $\omega_{GAM,0}(r_0)$ to the nonlinear GAM properties, we choose the ansatz $\omega_{GAM}(r, k_r) = \omega_{GAM,0}(r)(1 + \alpha k_r^2)$ for the dispersion relation. The resulting solution for k_r is $k_r(r) \approx \sqrt{1/(\alpha L_\omega(r_0))(r_0 - r)}$, where L_ω is the gradient length of $\omega_{GAM,0}$. Depending on the sign of α , k_r is imaginary on one side of the flux-surface at r_0 and real on the other, which implies the existence of a reflection layer at r_0 . Using the result for k_r and the condition $\dot{r} = \omega_{GAM,0}(r_0)/k_r$ for the phase velocity yields the curve of constant phase

$$t(r) = \frac{2}{3} \sqrt{-\frac{1}{\alpha L_\omega(r_0) \omega_{GAM,0}(r_0)}} (r - r_0)^{3/2} + t_0. \quad (1)$$

A least squares fit for the band-pass filtered flow profile in Fig. 1 c) with $\omega_{GAM,0}(r_0) = 0.98$ and the corresponding reference radius r_0 indicated by the dashed line yields $\alpha \approx 41\rho_s^2$, roughly a hundred times the value observed in the absence of turbulence ($|\alpha| \sim \rho_s^2/2$ [5]). Inserting the empirical finding $k_r\rho_s \lesssim 0.1$ into the expression for k_r , we can estimate the radial extent of a global eigenmode. For a linear dispersion relation $|\alpha| \sim \rho_s^2/2$, for a nonlinear dispersion $|\alpha| \sim 50\rho_s^2$. In tokamak edge plasmas $L_\omega \sim L_T \sim 0.01 \dots 0.1R$. Thus, assuming a major radius of $R \sim 2$ m, we obtain mode widths of $|r_0 - r| \lesssim 0.1 \dots 1$ mm and $1 \dots 10$ cm for nonlinear dispersions. Therefore, the width of nonlinear eigenmodes can be comparable to the scale length of the frequency plateaus reported in [1].

The turbulent source terms are particularly transparent if we write the time evolution of the GAM in terms of a state vector $\Psi \equiv (p_{GAM}, v_{GAM})$ as $\partial_t \Psi = \delta\Psi_{lin} + \delta\Psi_{nl}$. Here, p_{GAM} is the pressure and v_{GAM} the velocity component of the GAM. $\delta\Psi_{lin} \equiv (v_{GAM}, -p_{GAM})$ describes the linear time evolution and $\delta\Psi_{nl} \equiv (s_\Gamma, s_\Pi)$ the nonlinear source terms, where s_Π is the divergence of the Reynolds stress, and s_Γ the divergence of the turbulent transport. The energy stored in the GAM corresponds to the squared length of the state vector Ψ . Components of $\delta\Psi_{nl}$ changing the length of Ψ alter the energy, the components orthogonal to Ψ cause frequency shifts. A splitting of the nonlinear terms according to this idea for the Fourier mode with $\omega = 0.98$ [Fig. 1 c)] into energy inputs and frequency shifts shows that the observed frequency shift is due to the coupling to the up-down asymmetric component of the turbulent transport s_Γ alone, while the Reynolds stress does not contribute. A reduction of the resistivity results in reduced GAM group velocities, indicating a strong dependence of this effect on the ballooning character of the turbulence.

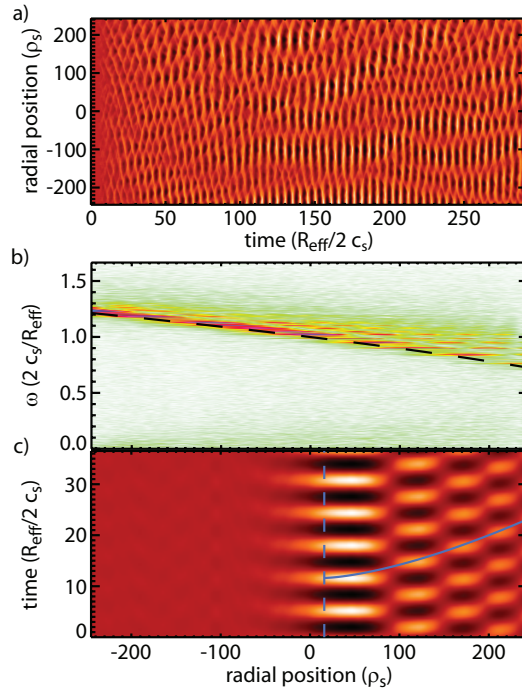


Figure 1: Non-local NLET turbulence study (slow parameter variation). a) Flux-surface averaged poloidal $\mathbf{E} \times \mathbf{B}$ velocity. b) Temporal Fourier transform (linear color scale) of a), local GAM frequency indicated by dashed line. c) Band-pass filtered flow profile at $\omega = 0.98$ with fit to curve of constant phase according to Eq. (1).

Pulsed GAM activity. We investigate the effect of up-down asymmetry of the magnetic geometry in local ITG edge-turbulence computations using upper and lower single-null geometries as described in [6] with the same parameters as in the previous paragraph but with adiabatic electrons. The striking difference between the two configurations is the asymmetry of the nonlinear GAM drive with respect to the sign of the phase velocity, which is obvious in the $\mathbf{E} \times \mathbf{B}$ -flow profiles in Fig. 2 a). Only GAMs with radially outward phase velocity are excited with the curvature drift directed away from the X-point whereas the phase velocity is radially inward with the curvature drift directed towards the X-point. The characteristic radial scale length of the GAMs is the same in both cases.

Including the frequency gradient in a nonlocal run, the GAM flow amplitude and the turbulence intensity become correlated and pulsed at a frequency much smaller than the GAM frequency [Fig. 2 b)]. The radial scale of the GAM in the initial phase ($t < 100$) is the same as in the local studies. The phase velocity is negative. However, due to the frequency gradient the wave fronts of the flows are being tilted in the $r - t$ -plane and k_r decreases. In response to the change of k_r the GAM amplitude and the turbulence intensity increase as if the shearing rate tends to adjust to its equilibrium value. For $k_r > 0$ the GAM is damped. After this burst of GAM intensity, the described cycle repeats. The pulse frequency obviously depends on the frequency gradient and on the initially growing wave number, i.e. $\omega_b \approx (2\pi/k_r)\partial_r\omega_{GAM,0}(r)$. Thus, a wide range of burst frequencies seems possible. For opposite sign of the ion curvature drift, the phase velocity is reversed and no pulsing is observed.

We investigate the dependence of the GAM-turbulence interaction on the sign of the phase velocity. Since we are not interested in the Reynolds stress here, we drop s_Π in the GAM equation above. The source term due to the turbulent transport Γ can be written as $s_\Gamma = -\partial_r\langle C(\theta)\Gamma \rangle$ in which the transport is modulated by the shearflow, $\Gamma \approx \hat{\Gamma}(\theta)v_{GAM}$ (for the Galilei invari-

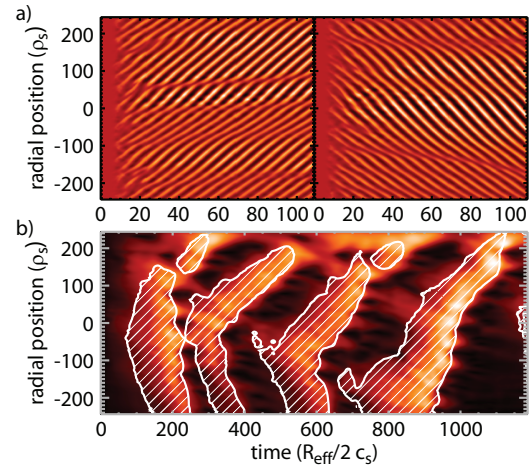


Figure 2: Flux-surface averaged poloidal $\mathbf{E} \times \mathbf{B}$ flows of local NLET ITG turbulence studies with a single-null geometry. a) Local runs. Left: Ion magnetic inhomogeneity drift v_d directed away from X-point. Right: v_d directed towards X-point. b) Non-local run and v_d towards X-point. Color-coded: short-time-RMS of $\mathbf{E} \times \mathbf{B}$ flow. Contours: turbulence intensity. Within the shaded areas, the turbulence intensity is above 70 % of its RMS average.

ance of this term see Ref. [7]). The poloidal structure of Γ is represented by $\hat{\Gamma}(\theta)$ and $C(\theta) \equiv \mathbf{v}_d \cdot (\nabla\Psi/|\nabla\Psi(\theta=0)|)/\langle \mathbf{v}_d \cdot (\nabla\Psi/|\nabla\Psi(\theta=0)|) \rangle$ (cf. [6]), where \mathbf{v}_d is the ion magnetic inhomogeneity drift velocity, Ψ the poloidal flux, and $\langle \dots \rangle$ the flux-surface average. Furthermore $\nu_{GAM} \approx -i(\omega_{GAM,0}/\omega_{GAM})p_{GAM}$, where $\omega_{GAM,0}$ is the linear, ω_{GAM} the (complex) nonlinear GAM frequency. Note that $\Re(\omega_{GAM}) \approx \omega_{GAM,0} = 1$ (due to normalization) and $\Re(\omega_{GAM}) \gg \Im(\omega_{GAM})$. With the expressions given above the aforementioned GAM equations yield the growth rate $\Im(\omega_{GAM}) \approx -k_r/2\langle C\hat{\Gamma} \rangle$. In up-down symmetric magnetic geometries $C(\theta)$ is up-down antisymmetric. Since empirically Γ is approximately symmetric with respect to the outboard midplane of the tokamak and positive, $\langle C\hat{\Gamma} \rangle = 0$ and the related growth rate is zero. However, in single-null geometry, $C(\theta)$ becomes very small close to the X-point. Hence, $\langle C\hat{\Gamma} \rangle \neq 0$. With the direction of ion magnetic drifts directed upwards – as is convention in NLET – and upper (lower) single-null geometry, $C(\theta)$ is positive (negative) opposite to the X-point. Thus, $\langle C\hat{\Gamma} \rangle$ becomes positive (negative), and the sign of the asymmetric growth rate $-(k_r/2)\langle C\hat{\Gamma} \rangle$ agrees with the GAM properties observed in Fig. 2 a).

Summary and Conclusions. The interaction with the turbulence can raise the group velocity of the GAM from the order of the curvature drift velocity (~ 0.1 km/s, $T \sim 100$ eV, $B \sim 1$ T, $R \sim 1$ m) in the linear case [5, 6] to the order of the diamagnetic drift velocity (~ 1 km/s), which is the typical scale of turbulent motions. A global nonlinear eigenmode can be wide enough to form frequency plateaus as observed in ASDEX Upgrade [1].

The pulsed GAM activity reported here is not unlikely to play a role in the explanation of the pulsed GAM activity observed recently in ASDEX Upgrade [2]. It can also serve as an approach to the understanding of the quiet periods in NSTX [3] alternative to the direct modulation of the turbulence activity by GAMs. Since the curvature drift was directed towards the X-point in all of the discharges analyzed in [3], it would be interesting to investigate the changes related to an inversion of the curvature drift.

References

- [1] G. D. Conway et al., *Plasma Physics and Controlled Fusion* **50**, 055009 (2008),
- [2] G. D. Conway et al., *Physical Review Letters* **106**, 065001, (2011),
- [3] S. Zweben et al., *Physics of Plasmas* **17**, 102502 (2010),
- [4] K. Hallatschek et al., *Physics of Plasmas* **7**, 2554-2564 (2000),
- [5] R. Hager, K. Hallatschek, *Physics of Plasmas* **16**, 072503 (2009),
- [6] R. Hager, K. Hallatschek, *Physics of Plasmas* **17**, 032112 (2010),
- [7] K. Hallatschek et al., *Physical Review Letters* **86**, 1223–1226 (2001).